Journal of Robotics and Control (JRC)
Volume 6, Issue 5, 2025
ISSN: 2715-5072, DOI: 10.18196/jrc.v6i5.27955

Adaptive Trajectory Control for Quadcopter using Extended Kalman Filter-Based Self-Tuning PID under Gaussian Disturbances

Belgis Ainatul Iza [1], Chairul Imron [2], Mardlijah [3*]
[1,2,3] Department of Mathematics, Institut Teknologi Sepuluh Nopember, Surabaya, Indonesia
Email: [1] belgisainatul@gmail.com, [2] cha_imron15@its.ac.id, [3] mardlijah@its.ac.id
*Corresponding Author

***Abstract*—Quadcopters are known for their maneuverability, but their stability is often challenged in changing environments. The PID parameters are adjusted manually so it is less adaptive. This research introduces the combination of Self-Tuning Proportional-Integral-Derivative (PID) and Extended Kalman Filter (EKF). A PID controller adjusts parameters based on errors and state estimates obtained from the EKF in real time. The disturbances used are Gaussian random disturbances on the system and sensors, simulated a normal distribution using the Simulink model. The basic PID parameters are determined through numerical simulations, then adaptively calibrated with a multiplier function based on estimation and error. The contributions of this study are: (1) developing an EKF-based Self-Tuning PID control for a quadcopter system; (2) demonstrating an adaptive response to disturbances through simulations; and (3) presenting an efficient tuning strategy suitable for resource-limited systems. From simulation, z-axis overshoot is successfully decreased from 7.37% to only 2.54%, while the steady-state error remains low under system disturbances. Computational efficiency is achieved because 12 state variables are controlled using a single set of global PID parameters, and the tuning process takes place in real time without relying on complex AI-based optimization methods. The proposed control approach is able to maintain trajectory tracking accuracy in three-dimensional space adaptively and with efficient resource usage. These results demonstrate that the EKF-PID method is effective for UAV control in dynamic and disruptive environments.**

Keywords*—Self-Tuning PID; Extended Kalman Filter; Quadcopter Control; Trajectory Tracking; Gaussian Disturbance

I. INTRODUCTION

The research of Unmanned Aerial Vehicles (UAVs) has enhanced significantly, especially quadcopters [1]–[3]. Quadcopters are systems that have 6 Degrees of Freedom (DOF) [4], [5], where the system is flexible and has high maneuverability. Therefore, quadcopters are widely applied in various fields, one of which is the delivery of goods [6]–[8]. According to [9], quadcopters are essential in modern logistics systems, especially in delivering goods in urban areas where congestion often occurs. However, the challenge that usually happens in quadcopter maneuvers is maintaining the accuracy of position and trajectory when environmental disturbances and changes occur [1]. A quadcopter is a non-linear system with coupled dynamics that requires high precision, so it is necessary to choose the proper control method to obtain optimal stability and performance.

PID is a conventional control that researchers often use to control quadcopters [10]–[15]. PID provides ease in design and implementation [16], [17]. These three PID controllers help each other by combining the K_i, K_p, and K_d values to obtain a stable output response and minimize oscillations at the set point [18]. Research by [19] showed that PID stabilizes quadcopters in introductory flight. However, the PID control method has weaknesses in parameter tuning [20], resulting in a limited ability to dampen disturbances in changing environmental conditions [1]. Several studies have been conducted to cope with the limitations of PID controllers. [21] optimized PID control based on machine learning for parameter tuning. [22] used an IBK-IFNN for PID parameter optimization. [23] also combined PID with Extreme Learning Machines (ELM) to track crack trajectories. Integration of PID and Machine Learning is also used in [24]–[26]. Although these methods can improve system response, they also have the potential to increase computational burden. A high computational burden without sufficient resources will be a challenge for lightweight systems such as quadcopters.

Various variants of PID controllers have also been developed in recent years, including sigmoid PID, BELBIC PID, and neuroendocrine PID. The use of these approaches offers more adaptive solutions, but in many cases, it is still not optimal for real systems with limited computational resources.

In addition, recent PID tuning methods, as shown by several recent studies [27]–[31], have demonstrated approaches based on artificial intelligence and evolutionary optimization. However, these approaches still require complex optimization and high computational duration. Therefore, a lighter, real-time, and robust PID tuning method is still needed in the face of external disturbances.

In addition to PID, several other control methods have

CC BY SA

been implemented on quadcopters by researchers. [32] applied active fault-tolerant control (AFTC) by combining RL and MPC for quadcopter trajectories with Actuator Errors. The study validated the control by simulating trajectory tracking. Although MPC can optimize motion based on the system model, it is computationally complex [33], which can be a constraint when applied to quadcopters with limited resources. [34] used CDBF, CLF, and TCBF to control the trajectory of Automated Vehicles, while [35] explored four variants of Sliding Mode Control (SMC) compared with three conventional controls to validate control tests for quadcopter trajectory tracking. Fuzzy Takagi-Sugeno (T-S) modeling presented by [36] demonstrated the efficiency of fuzzy control algorithms for quadcopter tracking with additional computational load analysis. Then, the methods of SMC and FSMC are compared by [37] for on AUV.

In this context, we propose the Extended Kalman Filter (EKF) and Self-Tuning PID combination as a method that can provide accurate state estimation and perform automatic control tuning. This approach overcomes the shortcomings of PID and AI methods with high computational burden.

Research related to the Extended Kalman Filter (EKF) on nonlinear dynamic systems has become the main focus of many studies. The study aims to improve the accuracy of estimation and control performance. [38] proved that EKF can provide good speed estimation results, so EKF is suitable for application in many fields, such as robots. The EKF also has the ability to adapt and has resilience in managing nonlinear systems [39] and handling disturbances and noise [40], [41]. Research by [42]–[44] combines fuzzy control and Kalman filter. Study in [45]–[47] introduced a more adaptive control using EKF to optimize fuzzy parameters and extract fuzzy rules while [48]–[51] discuss fuzzy adaptive unscented Kalman filter.

Research on control methods has been widely carried out by experts before, but it still has shortcomings and needs to be developed. Conventional PID has the advantage of producing a stable response in a predictable dynamic environment. Still, this method cannot adjust parameters automatically when environmental changes and disturbances occur. For MPC control, this approach performs well in position and trajectory control in a dynamic environment. However, the application of MPC to systems with high processing capabilities is minimal due to the significant computational cost. In applying the SMC technique, behind its effectiveness in producing a robust control response, this model still has a chattering effect that can interfere with performance in specific applications. Fuzzy control, often used to overcome high uncertainty, still has shortcomings in setting fuzzy parameters to define optimal rules [45], [52]. The method that has proven effective in improving state estimation, especially under uncertain conditions, is EKF [53]. The EKF approach is quite reliable, but real-time control adjustments under disturbances using the integration of EKF with Self-Tuning PID are still minimal. Hence, developing more adaptive control on quadcopters is still wide open.

The approach used in this study offers a real-time parameter adjustment process with minimal computational requirements. The proposed method does not require a machine learning-based iterative optimization process, but instead utilizes state estimation from the EKF to dynamically calibrate the PID parameters directly.

The key strength of this method is that it can control 12 state variables with only a single set of global PID parameters, thereby reducing calculation complexity and the risk of interactions between control channels. This study performs a conceptual comparison of the computational burden between the proposed method and commonly used AI-based approaches, and shows that our method remains adaptive to disturbances despite using more efficient computational resources.

Some important contribution points generated in this study are: (a) Developing an EKF-based Self-Tuning PID controller for a quadcopter system. (b) Demonstrating the adaptive control performance against external disturbances through numerical simulation. (c) Offers an efficient and less resource-intensive PID tuning as an alternative to current commonly used AI-based methods.

Organization of paper: Section I contains the introduction. The control algorithm of Self-Tuning PID based on EKF is explained in Section II. Next, section III provides the simulations and the results to prove the effectiveness of the quadcopter position and trajectory control. Last, section IV presents the conclusion.

II. METHOD

PID control is a conventional control that has three basic parameters, namely K_i, K_p, and K_d. In this study, PID control is combined with EKF to automatically adjust the three parameters. The Self-Tuning PID capability can improve control performance because it is more adaptive in responding to uncertain external disturbances. Self-tuning PID based on EKF is designed through several stages. First, input signal tracking is used to plan the position and trajectory. Second, EKF accurately estimates the system state and disturbance. Third, the EKF Estimator is combined with the Linear Quadratic Regulator (LQR) to obtain a more adaptive and efficient control system in controlling dynamic systems with high variability. Finally, PID effectively forms the variable of control u based on the error in the state. Fig. 1 presents the flow of the research methodology. The block diagram of the theoretical architecture is illustrated in Fig. 2, while Fig. 3 shows its actual implementation in Simulink, which integrates state space modeling, real-time state estimation, and adaptive PID control.

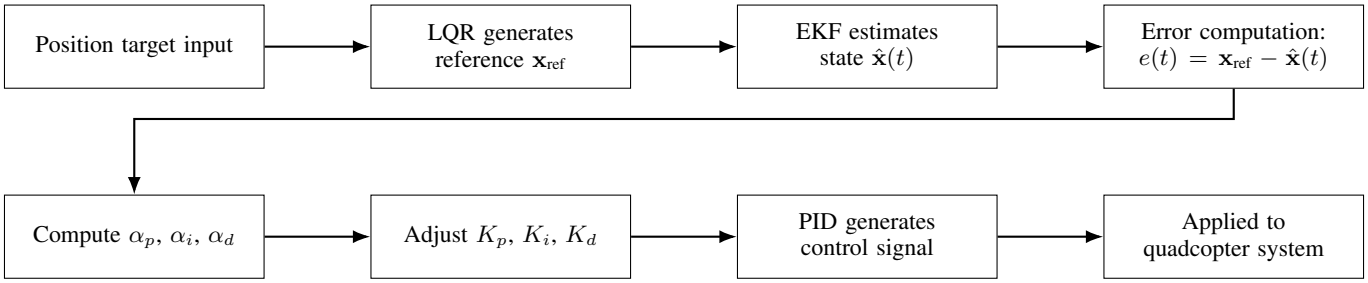

Fig. 1. Flowchart of The Proposed Control Methodology

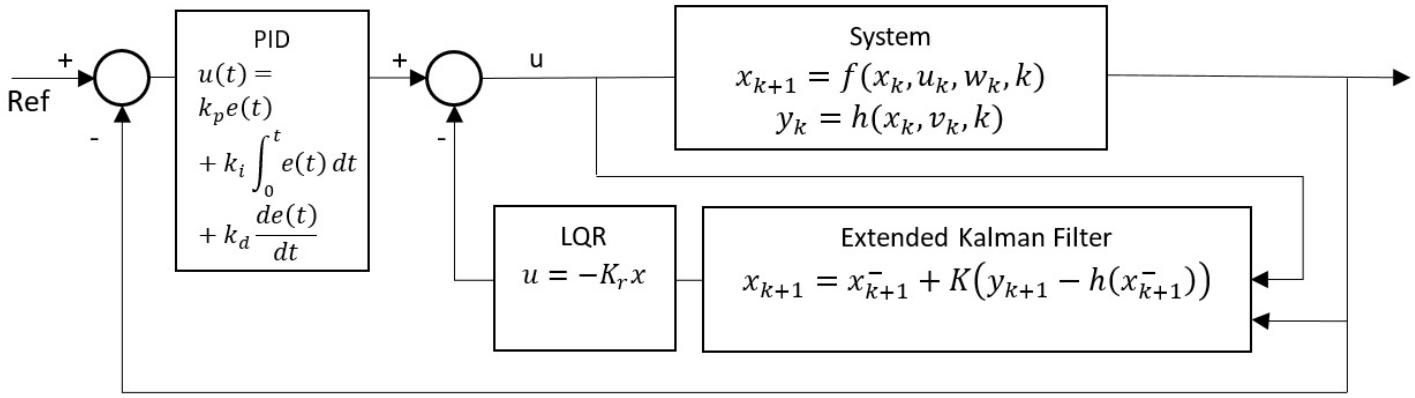

Fig. 2. Block Diagram of Self-Tuning PID based on EKF.

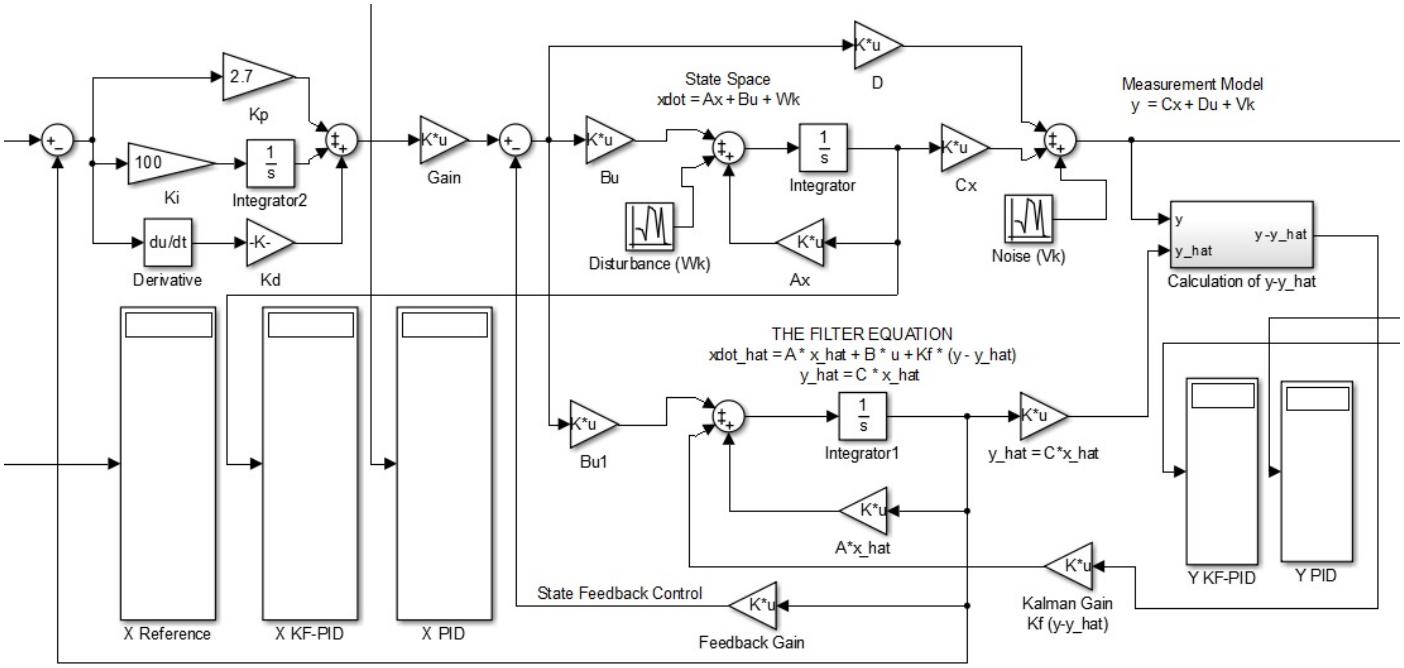

Fig. 3. Simulink Model of Self-Tuning PID based on EKF.

The plant used in this control system is a quadcopter with a 6-DOF dynamic model based on the Newton–Euler formulation. This model combines translational and rotational motions and is referenced from previously validated references [54]–[58]. The algorithms of each method are explained in the following sections.

A. Extended Kalman Filter

Kalman Filter is the estimator that minimizes the error between the estimated and actual values. By adding disturbance and measurement noise, the stochastic model of the state space is

$$\dot{x} = Ax + Bu + w_k, \tag{1}$$

$$y = Cx + Du + v_k. \tag{2}$$

The symbol w_k indicates the disturbance in the system representing the uncertainty of the model and v_k is the symbol of the measurement noise. With the Kalman Filter Estimator, the in Equation (1)- (2) can be specified as follows

$$\hat{\dot{x}} = A\hat{x} + Bu + K_f(y - \hat{y}), \tag{3}$$

$$\hat{y} = C\hat{x}, \tag{4}$$

where $\hat{x}$ is the estimated system state; y is output system expressed in Equation (2); the $\hat{y}$ notates the output of the estimated state, and K_f is the Kalman gain.

EKF is designed to handle dynamic systems whose models are nonlinear. In EKF, linearization is needed to obtain the A and H matrices used to calculate the covariance [59]. EKF works in two main steps, namely prediction and correction. The prediction step is used to estimate the variable of state, and the level of accuracy is calculated using the error covariance equation. In the correction step, the estimated results of the state variable are corrected using the measurement model. The Kalman gain matrix is used to minimize the error covariance. The predictions and corrections update steps will be repeated continuously until the k time iteration. Based on [59]–[64] the EKF algorithm is illustrated in Fig. 4.

LQR is an optimal control where the state equation is linear, the function is quadratic, and the test conditions include initial conditions without disturbance input [65]. The step after estimating the system state is to calculate the optimal control using the Linear Quadratic Regulator (LQR) method, where the feedback control is obtained from the LQR. This system applies LQR controller to generate optimal control signals from the state estimation result. The combination of EKF and LQR forms an optimal control architecture known as Linear Quadratic Gaussian (LQG), which is capable of handling nonlinear dynamic systems through accurate state estimation and optimal control.

Then, feedback control is designed using state error and integral feedback controller presented here [66]–[70]

$$u = -K_r x. \tag{5}$$

The gain K_r is the state feedback matrix gain. The feedback gain K_r of LQR is obtained using the `lqr()` function in MATLAB software, which solves the Riccati equation for a system in linear state-space form $\dot{x} = Ax + Bu$ by minimizing the quadratic cost function [66], [71]–[73]

$$J = \int_0^\infty \left(x^T Q x + u^T R u\right) dt. \tag{6}$$

The weight matrices Q and R are determined based on the priority between tracking precision and control energy efficiency. With the state estimation obtained from EKF and the optimal gain from LQR, the control system can provide a fast, stable, and efficient response in the face of external disturbances.

From the Equation (3)- (5), the new state space is obtained as follows

$$\hat{\dot{x}} = (A - BK_r - CK_f)\hat{x} + K_f y. \tag{7}$$

In this system, the LQR is not used as the main controller, but as a reference generator $x_{ref}(t)$ for the PID controller. The optimal trajectory is calculated from the linearized model of the system, then used as a reference input for the PID-EKF control system. Thus, LQR is used as a component in the trajectory planning stage, not as a direct controller of the actuator.

B. PID Parameter Tuning Strategy

PID control has strong performance under various operating conditions and has a simple structure [74]. The PID algorithm has three basic parameters, namely proportional, integral, and derivative. That means the control operates with error, integral error, and its derivative [18]. The PID parameter tuning process in this study is carried out through two main stages to improve control performance and system disturbance resilience. The first step in PID tuning is done with iterative tuning based on numerical simulation. The goal of this stage is to obtain initial parameters that provide system stability at nominal conditions before performing real-time adaptive tuning. The PID controller structure used refers to this equationc [74]–[80]

$$u(t) = K_p\ e(t) + K_i \int e(t)\ dt + K_d\ \frac{de(t)}{dt}. \tag{8}$$

To improve computational efficiency, the system uses a single set of PID parameters to control all 12 state variables. This approach is based on uniform sensitivity across variables so that the use of global gain maintains control accuracy. The more compact structure also reduces complexity and the risk of cross-channel interaction.

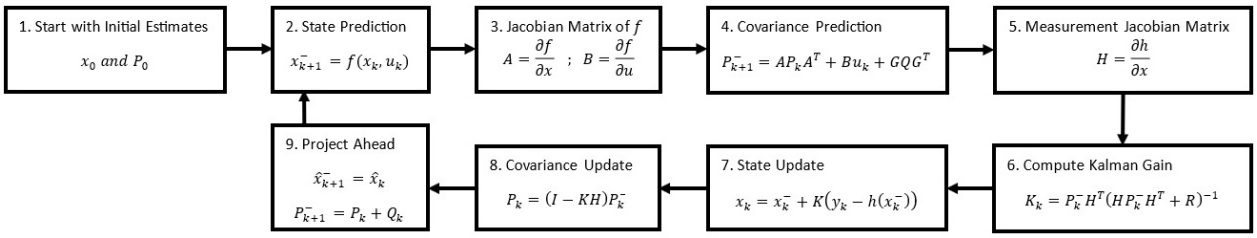

Fig. 4. EKF Algorithm Flowchart.

Even though the parameters used are global, the system remains adaptive to disturbances and changing conditions and is able to maintain good stability. The use of a single global set of PID parameters was chosen for computational efficiency reasons.

To maintain the performance of each channel and avoid cross-interaction, the tuning process is carried out adaptively through coefficients α that are dynamically adjusted to the error characteristics of each channel.

The basic PID parameters used in this study are $K_p = 2.7, K_i = 100, K_d = 0.0001$ obtained through simulation and evaluation of system performance against various disturbances. These values were chosen because they provide an optimal balance between rise time, overshoot, and stability, considering the characteristics of a 12-dimensional nonlinear quadcopter system and based on EKF estimation.

In the second stage, a real-time adaptive self-tuning mechanism is performed using error information obtained from the Extended Kalman Filter (EKF). In this stage, the initial PID parameters are recalibrated based on the system conditions while running. The final values of the PID parameters are formulated as

$$K_p^{final} = K_p^{basic} \cdot \alpha_p(t), \tag{9}$$

$$K_i^{final} = K_i^{basic} \cdot \alpha_i(t), \tag{10}$$

$$K_d^{final} = K_d^{basic} \cdot \alpha_d(t), \tag{11}$$

where $\alpha_p(t), \alpha_i(t), \alpha_d(t)$ act as an adaptive adjustment coefficient obtained from the deviation between the estimated state by EKF and the expected reference value. The $\alpha_j(t)$ value is obtained from this equation

$$\alpha_j(t) = 1 + \beta_j \cdot |e_j(t)|, \quad j \in \{p, i, d\}, \tag{12}$$

where $e_j(t)$ declare error at t and β_j is the sensitivity constant obtained through initial numerical simulations. Thus, the control system can adjust its control parameters dynamically to respond to disturbances or changes in system parameters.

This combined approach of offline numerical tuning and online adaptive adjustment results in a robust and responsive control strategy suitable for application to multivariable nonlinear systems such as quadcopters.

III. Results and Discussion

The simulation have been designed to handle the stability of the quadcopter. The target position and trajectory in this study are circle on a horizontal plane. To obtain a more accurate simulation, disturbance variables are involved. The simulation data analyzed are angular position, angular velocity, linear position, linear velocity, and trajectory tracking in 3-dimensional space. The performance comparison between the EKF-PID controller and the conventional PID, both under undisturbed and disturbed conditions, is presented in Table I. The system response of angular and translational are presented in Fig. 5- 7, while the trajectory tracking is illustrated in Fig. 8.

The control performance improvements shown in Table I stem from an adaptive tuning mechanism based on state estimation by the EKF. When disturbances or dynamic changes occur, the error value increases, and the adaptive coefficients α_p, α_i, and α_d are automatically adjusted to account for the error. This enables faster and more stable control response without the need for manual tuning or complex computations. Thus, the improved performance in RMSE and computation time is a direct result of integrating EKF estimation with real-time PID tuning.

The improvement in system performance is closely related to the implementation of the EKF, which has been proven to maintain low RMSE values across all state variables. The accuracy of the state estimation from the EKF helps the PID adjust its parameters according to the current system conditions. This is supported by the data in Table I, where the average RMSE values using the EKF-PID are each smaller than those obtained from the conventional PID. This finding demonstrates that state information from the EKF is an important foundation in the parameter tuning process, resulting in faster response and more accurate control in following the trajectory.

Fig. 5 shows the system response of the roll, pitch, and yaw angular positions under disturbance. The Fig. 5a indicates that the roll steady state remains low even though there is a disturbance, which is 0.27%. It also happens on pitch position on Fig. 5b which has only 0.07%. It means that the designed controller can respond well to system dynamics. For the yaw position, described in Fig. 5c, the overshoot increased from 0% to 22.66% when given a disturbance.

TABLE I. COMPARISON OF EKF-PID AND PID

Variable	Control	Without Disturbance				With Disturbance			
		Settling Time (s)	Rise Time (s)	ISE	SSE	Settling Time (s)	Rise Time (s)	ISE	SSE
Roll	EKF-PID	14.97	0.00	1.5096	0.00587	–	0.00	1.5133	0.02325
	PID	14.95	0.00	1.5888	0.00169	14.99	0.00	1.5961	0.01850
Roll Velocity	EKF-PID	–	0.00	10.053	0.37230	–	0.00	10.4065	0.53881
	PID	–	0.00	11.7051	0.37203	–	0.00	12.1129	0.55162
Pitch	EKF-PID	–	0.00	1.0293	0.37228	–	0.00	1.0666	0.42102
	PID	–	0.00	1.0340	0.37203	–	0.00	1.0797	0.42716
Pitch Velocity	EKF-PID	14.96	0.00	1.5089	0.00401	–	0.00	3.0535	0.15019
	PID	14.94	0.00	1.5881	0.00017	–	0.00	3.0386	0.18043
Yaw	EKF-PID	2.03	1.13	0.06685	1.19e-13	–	0.79	0.08180	0.03940
	PID	1.79	0.98	0.07288	1.74e-10	–	0.77	0.09084	0.04540
Yaw Velocity	EKF-PID	1.95	0.00	0.24877	2.29e-13	–	0.00	0.32437	0.12598
	PID	1.94	0.00	0.24556	1.90e-14	–	0.00	0.29665	0.11544
X Position	EKF-PID	–	0.90	75.2235	1.0502	–	0.92	77.0145	1.1613
	PID	–	0.88	73.4328	1.0482	–	0.90	75.1724	1.1613
X Velocity	EKF-PID	–	0.00	91.5476	0.0759	–	0.00	92.8431	0.1315
	PID	14.99	0.00	91.4677	0.0348	–	0.00	92.7979	0.0946
Y Position	EKF-PID	–	0.76	86.5047	3.1329	–	0.84	86.7491	3.2004
	PID	–	0.77	84.5752	3.0918	–	0.84	84.8016	3.1579
Y Velocity	EKF-PID	–	0.00	99.0573	3.6517	–	0.00	99.2904	3.7359
	PID	–	0.00	99.5099	3.6495	–	0.00	99.7535	3.7390
Z Position	EKF-PID	7.37	4.10	23.8126	0.00175	13.89	3.82	23.1818	0.02147
	PID	7.62	2.85	34.6704	0.00099	14.41	2.67	33.7201	0.03712
Z Velocity	EKF-PID	6.49	0.00	7.9845	0.00092	14.92	0.00	7.8119	0.06719
	PID	9.04	0.00	6.6685	0.00121	–	0.00	6.6704	0.09676

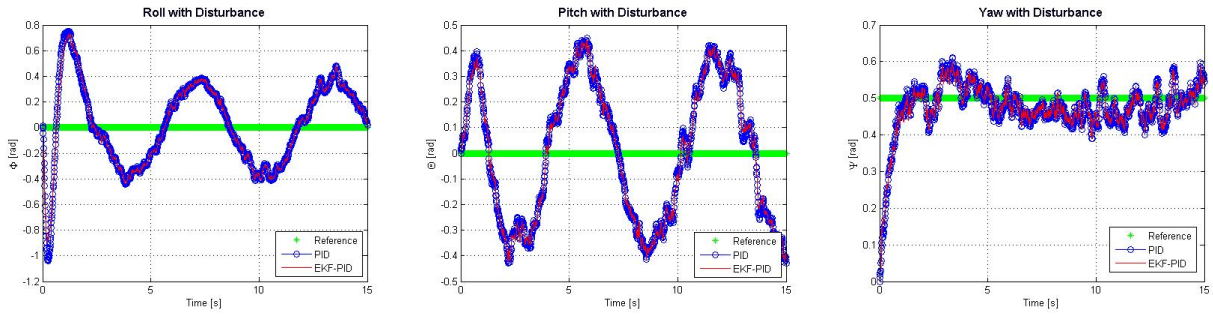

(a) (b) (c)

Fig. 5. Angular Position Response with Disturbance: (a) Roll, (b) Pitch, (c) Yaw.

The increased overshoot needs to be overcome by reducing the initial fluctuation. However, the steady-state error of the yaw position is excellent even though there is a disturbance, which remains at a percentage of 0.06%, which indicates that the control can maintain stability for a long duration.

The stability of the angular velocity is shown in Fig. 6. The Fig. 6a shows a slight increase in the steady-state error of the roll angular velocity, which is from 0.10% to 0.14%. Although there is an increase in the roll angular velocity, the steady-state error is still within the tolerance limit under the disturbance. Fig. 6b present pitch angular velocity, which decreases from 0.36% to 0.18%. For the yaw angular velocity, illustrated in Fig. 6c, it can be seen in the figure that the steady state error is zero percent and only increases by 0.09% when subjected to disturbance.

Linear position response to three axes is shown in Fig. 7. Although the settling time of the x-axis increases when disturbed, shown in Fig. 7a, from 0.28 seconds to 4 seconds, the steady-state error remains at 2.71%. These results indicate that the control system can achieve stability even though it takes a little longer after the disturbance. While on Fig. 7b, the steady-state error of the y-axis is reduced from 1.90% to 1.81% which proves that the system can adapt to changes in disturbance. In on Fig. 7c, a significant decrease in overshoot happens on the z-axis, from 7.37% to 2.54%. Besides, the z-axis also maintains a small steady-state error, that is, 0.03%. This decrease reflects that the control system has been optimal in maintaining height. Furthermore, the steady state error of linear velocity is low; the maximum value is 3.14%, which occurs when the x-axis velocity is disturbed. The adaptive coefficient $\alpha_p(t), \alpha_i(t), \alpha_d(t)$ directly affects the control response to disturbances when applied to the system. When the deviation between the estimated state and the reference is large.

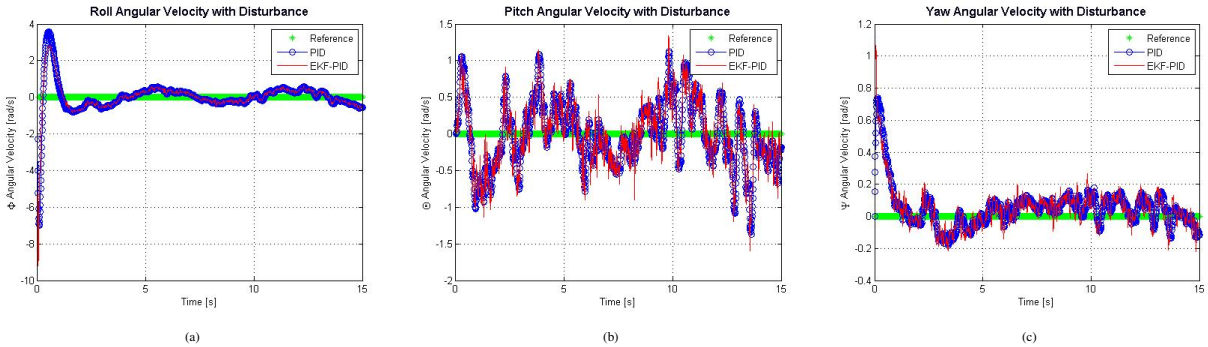

Fig. 6. Angular Velocity Response with Disturbance: (a) Roll, (b) Pitch, (c) Yaw.

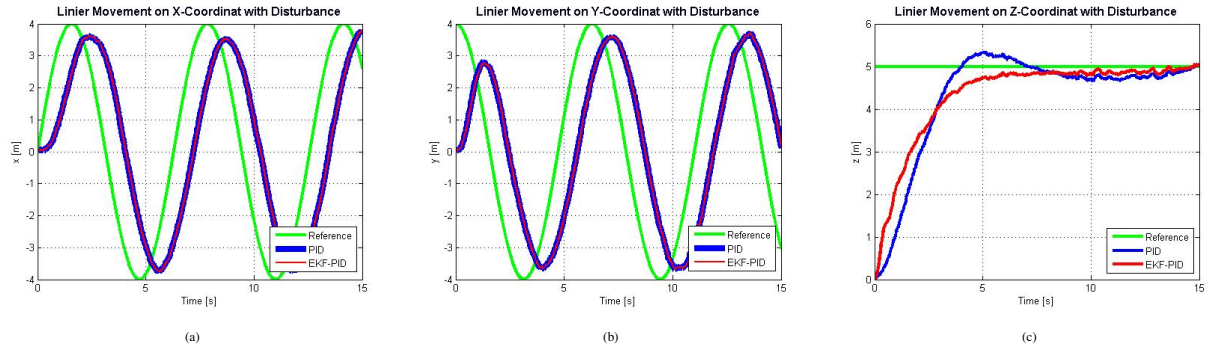

Fig. 7. Linear Position Response with Disturbance: (a) x, (b) y, (c) z.

The value of α increases, resulting in rapid error correction. This is evident from the decreasing in z-axis overshoot, from 7.37% to 2.54%. Furthermore, the yaw value remains stable despite the Gaussian disturbances. Thus, real-time tuning by means of α can reduce overshoot and maintain the precision of trajectory tracking.

The quadcopter trajectory graph in three-dimensional space is illustrated in Fig. 8. It shows that Fig. 8a simulates trajectory tracking on three dimensions, which compares PID control and self-tuning PID based on EKF without disturbance. While the trajectory tracking with disturbance is described in Fig. 8b. In this figure, the quadcopter can follow the trajectory according to the desired reference despite interference. This performance proves that the designed control system, namely the integration of EKF estimation with PID parameter tuning, can respond adaptively and robustly.

Previous studies have explored the integration of Extended Kalman Filter (EKF) or fuzzy logic approaches in PID control for UAV systems. [42]–[44] combined the EKF with a fuzzy-based tuning scheme to improve control performance. However, this approach requires a relatively complex computational process and a complex tuning process. In contrast, the system proposed in this study uses a set of global PID parameters that are adjusted in real time through an adaptive multiplier function based on the error and the EKF estimation results. With this approach, simulation results show that the z-axis overshoot is successfully reduced from 7.37% to 2.54%, and the steady-state error at a fixed position is below 0.06 in simulation units. In this study, the method is able to achieve competitive performance without relying on data training processes or AI-based optimization algorithms. This makes the proposed method computationally lighter to implement in UAV systems with hardware limitations. Based on the comparison results, the EKF-PID shows an adaptive response and an accuracy in following the trajectory.

The EKF-PID control approach successfully demonstrated significant improvements in suppressing overshoot and maintaining low steady-state errors, but performance on the yaw axis still exhibited relatively larger oscillations compared to other channels. This is because the yaw characteristic is more susceptible to external disturbances and interactions between rotational channels. The yaw fluctuation interferes with the stability of direction. Therefore, more specific parameter tuning focused on the yaw is needed to ensure reliability under complex conditions.

Although no direct quantitative comparisons have been conducted with other AI-based control or optimization methods, the system is designed to be computationally efficient. This is because it uses only a single set of global PID parameters to control all 12 state variables.

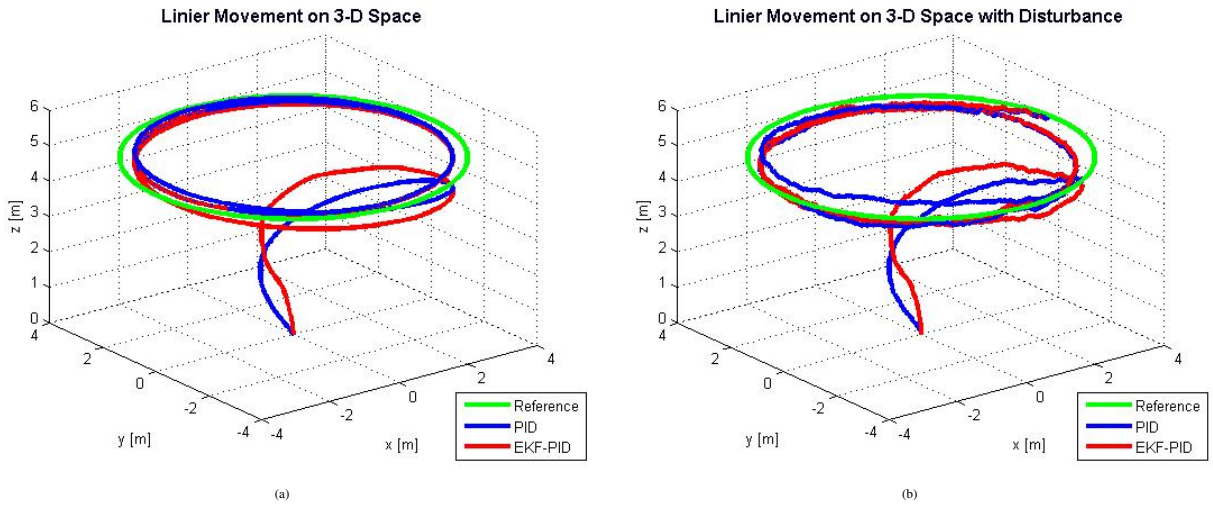

Fig. 8. Trajectory Tracking on 3D: (a) Without Disturbance, (b) With Disturbance.

This approach eliminates specific parameter tuning for each channel, reducing the computational burden, especially in resource-constrained systems. This research was conducted in a simulated environment with Gaussian noise representing system and sensor noise. Other types of noise, such as permanent bias, actuator delay, or aerodynamic turbulence, have not been tested.

Furthermore, validation on a real UAV platform has not been performed. Therefore, hardware testing is necessary in future research. Some important results that prove the proposed control effectiveness are

- The EKF-PID control system successfully reduced the overshoot on the z-axis from 7.37% to 2.54%, as shown in Table I.
- Under Gaussian disturbances, the average steady-state error remains below 0.1 rad for roll, pitch, and yaw, indicating system stability.
- Fig. 8 shows that the actual trajectory follows the set point, with a maximum position deviation of < 0.15 m on the x-axis and < 0.2 m on the y-axis.
- Although no runtime measurements have been performed, computational efficiency is indicated by the successful control of 12 state variables using a set of global PID parameters, without an AI-based optimization algorithm.

IV. Conclusion

In this study, an adaptive quadcopter control system is successfully developed by integrating a Self-Tuning PID controller based on the EKF. The proposed method is able to adjust control parameters in real-time based on the estimated system state so that it can maintain high stability performance even in changing environmental conditions or containing disturbances.

Quantitatively, the EKF-PID system was able to reduce the z-axis overshoot from 7.37% to 2.54% and maintain steady-state position errors below 0.1 meters for all translation axes. Based on the simulation, the RMSE values of x, y, and z positions are 0.0527, 0.0491, and 0.0432, respectively. Furthermore, there was a small oscillation in the yaw response. However, the yaw response remained within tolerance limits. It prove the successful of adaptive tuning for rotation.

The system's computational advantage lies in the use of a single set of global PID parameters for 12 state variables, with adaptive tuning based on the EKF's estimated error. The number of blocks and simulation time indicate that the system can run stably at real-time processing speeds in MATLAB Simulink without overloading.

This method has the potential to serve as a foundation for the development of state estimation-based adaptive control in the future. However, this system is limited by oscillations in the yaw channel and relies heavily on initial parameter selection through numerical simulation. In addition, the types of disturbances tested are still limited to Gaussian distributions, so further testing on real disturbance scenarios such as wind turbulence or load variations is recommended.

Acknowledgement

The authors acknowledge the support from the Department of Mathematics, Institut Teknologi Sepuluh Nopember, and from the IMU-CDC through the GRAID Program.

References

[1] X. Chang, C. Jin, and Y. Cheng, "Dynamics and advanced active disturbance rejection control of tethered uav," *Applied Mathematical Modelling*, vol. 135, pp. 640–665, 2024, doi: 10.1016/j.apm.2024.07.011.

[2] R. Guo, W. Guo, B. Chang, and L. Long, "Safety-critical control of planar quadcopters under dynamic event-triggered mechanism," *Journal of the Franklin Institute*, vol. 361, no. 9, 2024, doi: 10.1016/j.jfranklin.2024.106886.

[3] P. C. Yuste, J. A. I. Martínez, and M. A. S. de Miguel, "Simulation-based evaluation of model-free reinforcement learning algorithms for quadcopter attitude control and trajectory tracking," *Neurocomputing*, vol. 608, 2024, doi: 10.1016/j.neucom.2024.128362.

[4] A. Modi, N. Joshi, and A. Mehta, "Robust discrete-time super twisting formation protocol for a 6-dof quadcopter swarm," *ISA transactions*, vol. 143, pp. 177–187, 2023, doi: 10.1016/j.isatra.2023.09.029.

[5] V. Biazi, J. Nedoma, and C. Marques, "Trajectory tracking and state estimation for quadcopter uavs using particle filters in an inner-outer loops controller," *Expert Systems with Applications*, vol. 296, no. Part D, 2026, doi: 10.1016/j.eswa.2025.129245.

[6] F. Ahmad, P. Kumar, P. P. Patil, R. Dobriyal, and S. Avikal, "Comparative analysis of two and four blades quadcopter propellers based on finite element method," *Materials Today: Proceedings*, 2023, doi: 10.1016/j.matpr.2023.07.050.

[7] M. E. Guerrero-Sánchez, R. Lozano, P. Castillo, O. Hernández-González, C. García-Beltrán, and G. Valencia-Palomo, "Nonlinear control strategies for a uav carrying a load with swing attenuation," *Applied Mathematical Modelling*, vol. 91, pp. 709–722, 2021, doi: 10.1016/j.apm.2020.09.027.

[8] M. A. Mafaz, N. Horri, Q. Lu, and M. England, "Robust auto-tuning control of a delivery quadcopter with motor faults, mass and inertia estimation," *IFAC-PapersOnLine*, vol. 58, no. 28, pp. 744–749, 2024, doi: 10.1016/j.ifacol.2025.01.055.

[9] A. Gupta, T. Afrin, E. Scully, and N. Yodo, "Advances of uavs toward future transportation: The state-of-the-art, challenges, and opportunities," *Future transportation*, vol. 1, no. 2, pp. 326–350, 2021, doi: 10.3390/futuretransp1020019.

[10] I. Trenev, A. Tkachenko, and A. Kustov, "Movement stabilization of the parrot mambo quadcopter along a given trajectory based on pid controllers," *IFAC-PapersOnLine*, vol. 54, no. 13, pp. 227–232, 2021, doi: 10.1016/j.ifacol.2021.10.450.

[11] S. B. Abdi, A. Debilou, L. Guettal, and A. Guergazi, "Robust trajectory tracking control of a quadrotor under external disturbances and dynamic parameter uncertainties using a hybrid p-pid controller tuned with ant colony optimization," *Aerospace Science and Technology*, vol. 160, 2025, doi: 10.1016/j.ast.2025.110053.

[12] A. Gün, "Attitude control of a quadrotor using pid controller based on differential evolution algorithm," *Expert Systems with Applications*, vol. 229, 2023, doi: 10.1016/j.eswa.2023.120518.

[13] I. Lopez-Sanchez and J. Moreno-Valenzuela, "Pid control of quadrotor uavs: A survey," *Annual Reviews in Control*, vol. 56, 2023, doi: 10.1016/j.arcontrol.2023.100900.

[14] S. Wang, A. Polyakov, and G. Zheng, "Quadrotor stabilization under time and space constraints using implicit pid controller," *Journal of the Franklin Institute*, vol. 359, no. 4, pp. 1505–1530, 2022, doi: 10.1016/j.jfranklin.2022.01.002.

[15] J. A. Cárdenas, U. E. Carrero, E. C. Camacho, and J. M. Calderón, "Optimal pid ø axis control for uav quadrotor based on multi-objective pso," *IFAC-PapersOnLine*, vol. 55, no. 14, pp. 101–106, 2022, doi: 10.1016/j.ifacol.2022.07.590.

[16] M. Jalilian, A. Rastgou, S. Kharrati, and S. Hosseini-Hemati, "Load frequency control resilience of hybrid power system with renewable energy sources and superconducting magnetic energy storage using fo-fuzzy-pid controller," *Results in Engineering*, vol. 27, 2025, doi: 10.1016/j.rineng.2025.105961.

[17] X. Guo, Z. Lin, D. Yang, Y. Yang, L. Jiang, and Y. Liu, "Experimental evaluation on pid-based adaptive longitudinal ventilation control of tunnel fire smoke," *Journal of Wind Engineering and Industrial Aerodynamics*, vol. 254, 2024, doi: 10.1016/j.jweia.2024.105884.

[18] H. A. Issa, L. M. Abdali, H. Alhusseini, and V. I. Velkin, "Design, modeling, and control of a dual-axis solar tracker using fractional order pid controllers for enhanced energy efficiency," *Results in Engineering*, vol. 27, 2025, doi: 10.1016/j.rineng.2025.106073.

[19] J. Yoon and J. Doh, "Optimal pid control for hovering stabilization of quadcopter using long short term memory," *Advanced Engineering Informatics*, vol. 53, 2022, doi: 10.1016/j.aei.2022.101679.

[20] K. Liu, Y. Fan, and J. Chen, "A model free adaptive control method based on self-adjusting pid algorithm in ph neutralization process," *Chinese Journal of Chemical Engineering*, vol. 76, pp. 227–236, 2024, doi: 10.1016/j.cjche.2024.09.005.

[21] L. Yan, J. L. Webber, A. Mehbodniya, B. Moorthy, S. Sivamani, S. Nazir, and M. Shabaz, "Distributed optimization of heterogeneous uav cluster pid controller based on machine learning," *Computers and Electrical Engineering*, vol. 101, 2022, doi: 10.1016/j.compeleceng.2022.108059.

[22] X. Gong, X. Wang, W. Xiong, H. Zhang, and Y. Xin, "An effective pid control method of air conditioning system for electric drive workshop based on ibk-ifnn two-stage optimization," *Journal of Building Engineering*, vol. 98, 2024, doi: 10.1016/j.jobe.2024.111028.

[23] J. Zhang, X. Yang, W. Wang, I. Brilakis, D. Davletshina, and H. Wang, "Robust elm-pid tracing control on autonomous mobile robot via transformer-based pavement crack segmentation," *Measurement*, vol. 242, 2025, doi: 10.1016/j.measurement.2024.116045.

[24] G. Reynoso-Meza, J. Carrillo-Ahumada, and T. Marques, "Multi-objective machine learning for control performance assessment in pid control loops," *IFAC-PapersOnLine*, vol. 58, no. 7, pp. 168–173, 2024, doi: 10.1016/j.ifacol.2024.08.029.

[25] L. Wang, Y. Cheng, G. Parekh, and R. Naidu, "Real-time monitoring and predictive analysis of voc flux variations in soil vapor: Integrating pid sensing with machine learning for enhanced vapor intrusion forecasts," *Science of The Total Environment*, vol. 924, 2024, doi: 10.1016/j.scitotenv.2024.171616.

[26] S. Saat, M. A. Ahmad, and M. R. Ghazali, "Data-driven brain emotional learning-based intelligent controller-pid control of mimo systems based on a modified safe experimentation dynamics algorithm," *International Journal of Cognitive Computing in Engineering*, vol. 6, pp. 74–99, 2025, doi: 10.1016/j.ijcce.2024.11.005.

[27] N. F. Nanyan, M. A. Ahmad, and B. Hekimoğlu, "Optimal pid controller for the dc-dc buck converter using the improved sine cosine algorithm," *Results in Control and Optimization*, vol. 14, 2024, doi: 10.1016/j.rico.2023.100352.

[28] M. Moučka and M. Hofreiter, "PID Controller With an Autotuning Function," in *IEEE Access*, vol. 12, pp. 136202-136221, 2024, doi: 10.1109/ACCESS.2024.3462090.

[29] L. Ramos-Velasco, V. Parra-Vega, R. García-Rodríguez, M. Vega-Navarrete, C. Trejo-Ramos, and E. Olguín-Díaz, "Knowledge-based self-tuning of pid control gains for continuum soft robots," *Engineering Applications of Artificial Intelligence*, vol. 133, 2024, doi: 10.1016/j.engappai.2024.108447.

[30] M. Z. M. Tumari, M. A. Ahmad, and M. I. M. Rashid, "A fractional order pid tuning tool for automatic voltage regulator using marine predators algorithm," *Energy Reports*, vol. 9, pp. 416–421, 2023, doi: 10.1016/j.egyr.2023.10.044.

[31] R. S. Patil, S. P. Jadhav, and M. D. Patil, "Review of intelligent and nature-inspired algorithms-based methods for tuning pid controllers in industrial applications," *Journal of Robotics and Control (JRC)*, vol. 5, no. 2, pp. 336–358, 2024, doi: 10.18196/jrc.v5i2.20850.

[32] H. Jiang, F. Xu, X. Wang, and S. Wang, "Active fault-tolerant control based on mpc and reinforcement learning for quadcopter with actuator faults," *IFAC-PapersOnLine*, vol. 56, no. 2, pp. 11853–11860, 2023, doi: 10.1016/j.ifacol.2023.10.589.

[33] H. Xiong, L. Xie, C. Hu, and H. Su, "A fuzzy compensation-koopman mpc design for pressure regulation in pem electrolyzer," *Chinese Journal of Chemical Engineering*, vol. 76, pp. 251–263, 2024, doi: 10.1016/j.cjche.2024.09.004.

[34] J. Meng, J. Zhao, and Y. Chen, "Reinforcement learning enabled safety-critical tracking of automated vehicles with uncertainties via integrated control-dependent, time-varying barrier function, and control lyapunov function," *IFAC-PapersOnLine*, vol. 56, no. 3, pp. 85–90, 2023, doi: 10.1016/j.ifacol.2023.12.005.

[35] A. Mughees, I. Ahmad, N. Mughees, and A. Mughees, "Conditioned adaptive barrier-based double integral super twisting smc for trajectory tracking of a quadcopter and hardware in loop using igwo algorithm," *Expert Systems with Applications*, vol. 235, 2024, doi: 10.1016/j.eswa.2023.121141.

[36] M. S. Aslam and H. Bilal, "Modeling a takagi-sugeno (ts) fuzzy for un-

manned aircraft vehicle using fuzzy controller," *Ain Shams Engineering Journal*, vol. 15, no. 10, 2024, doi: 10.1016/j.asej.2024.102984.

[37] Mardlijah, Y. F. Akbar and B. A. Iza, " Comparative Analysis of SMC and FSMC on Autonomous Underwater Vehicle (AUV) with Active Ballast," *2023 International Conference on Computer, Control, Informatics and its Applications (IC3INA)*, pp. 7-12, 2023, doi: 10.1109/IC3INA60834.2023.10285788.

[38] M. Megrini, A. Gaga, Y. Mehdaoui, and J. Khyat, "Design and pil test of extended kalman filter for pmsm field oriented control," *Results in Engineering*, vol. 24, 2024, doi: 10.1016/j.rineng.2024.102843.

[39] L. Rosafalco, P. Conti, A. Manzoni, S. Mariani, and A. Frangi, "Ekf–sindy: Empowering the extended kalman filter with sparse identification of nonlinear dynamics," *Computer Methods in Applied Mechanics and Engineering*, vol. 431, 2024, doi: 10.1016/j.cma.2024.117264.

[40] H. Shiri, P. Zimroz, A. Wyłomańska, and R. Zimroz, "Estimation of machinery's remaining useful life in the presence of non-gaussian noise by using a robust extended kalman filter," *Measurement*, vol. 235, 2024, doi: 10.1016/j.measurement.2024.114882.

[41] L. Jiang and L. Wu, "Enhanced yolov8 network with extended kalman filter for wildlife detection and tracking in complex environments," *Ecological Informatics*, vol. 84, 2024, doi: 10.1016/j.ecoinf.2024.102856.

[42] R. Sajedi, J. Faraji, F. Kowsary, and A. Kahrbaeiyan, "Estimation of thermal parameters of a locomotive brake disc using an adaptive type 1 and type 2 fuzzy kalman filter," *International Communications in Heat and Mass Transfer*, vol. 157, 2024, doi: 10.1016/j.icheatmasstransfer.2024.107825.

[43] D. Liu, S. Wang, Y. Fan, C. Fernandez, and F. Blaabjerg, "A novel multi-factor fuzzy membership function-adaptive extended kalman filter algorithm for the state of charge and energy joint estimation of electric-vehicle lithium-ion batteries," *Journal of Energy Storage*, vol. 86, 2024, doi: 10.1016/j.est.2024.111222.

[44] C. Xu, E. Zhang, K. Jiang, and K. Wang, "Dual fuzzy-based adaptive extended kalman filter for state of charge estimation of liquid metal battery," *Applied Energy*, vol. 327, 2022, doi: 10.1016/j.apenergy.2022.120091.

[45] H. Taghavifar, "Ekf estimation based pid type-2 fuzzy control of electric cars," *Measurement*, vol. 173, 2021, doi: 10.1016/j.measurement.2020.108557.

[46] D. C. dos Santos Gomes and G. L. de Oliveira Serra, "Interval type-2 evolving fuzzy kalman filter for processing of unobservable spectral components from uncertain experimental data," *Journal of the Franklin Institute*, vol. 361, no. 2, pp. 637–669, 2024, doi: 10.1016/j.jfranklin.2023.12.017.

[47] H. Samet, S. Ketabipour, and N. Vafamand, "Ekf-based ts fuzzy prediction for eliminating the extremely fast reactive power variations in manjil wind farm," *Electric Power Systems Research*, vol. 199, 2021, doi: 10.1016/j.epsr.2021.107422.

[48] S. Mokhtari and K. K. Yen, "Dynamic state estimation with additive noise for load frequency control using bilateral fuzzy adaptive unscented kalman filter," *Electric Power Systems Research*, vol. 220, 2023, doi: 10.1016/j.epsr.2023.109363.

[49] M. Kumar and S. Mondal, "Advancements and prospects of fuzzy-based adaptive unscented kalman filters for nonlinear systems: A review," *Applied Soft Computing*, vol. 177, 2025, doi: 10.1016/j.asoc.2025.113297.

[50] J. Faraji, J. Keighobadi, and F. Janabi-Sharifi, "Design and implementation of an adaptive unscented kalman filter with interval type-3 fuzzy set for an attitude and heading reference system considering gyroscope bias," *Mechanical Systems and Signal Processing*, vol. 223, 2025, doi: 10.1016/j.ymssp.2024.111870.

[51] M. A. A. Varzaneh and M. Mohammadi, "A novel fuzzy adaptive unscented kalman filter for model updating using biased measurements," *Mechanical Systems and Signal Processing*, vol. 230, 2025, doi: 10.1016/j.ymssp.2025.112519.

[52] D. Acharya, A. Rai, and D. K. Das, "Optimal rule based fuzzy-pi controller for core power control of nuclear reactor," *Annals of Nuclear Energy*, vol. 194, 2023, doi: 10.1016/j.anucene.2023.110118.

[53] V. H. Matthias *et al.*, "Physics-informed ensembles of dual extended kalman filters for online state and parameter estimation of mechatronic systems," *Mechanical Systems and Signal Processing*, vol. 229, 2025, doi: 10.1016/j.ymssp.2025.112469.

[54] M. A. Sadi, A. Jamali, A. M. N. bin Abang Kamaruddin, and V. Y. S. Jun, "Cascade model predictive control for enhancing uav quadcopter stability and energy efficiency in wind turbulent mangrove forest environment," *e-Prime-Advances in Electrical Engineering, Electronics and Energy*, vol. 10, 2024, doi: 10.1016/j.prime.2024.100836.

[55] A. Nikhilraj, H. Simha, and H. Priyadarshan, "Modeling and control of port dynamics of a tilt-rotor quadcopter," *IFAC-PapersOnLine*, vol. 55, no. 1, pp. 746–751, 2022, doi: 10.1016/j.ifacol.2022.04.122.

[56] E. Chnib, P. Bagnerini, and A. Zemouche, "Lmi based h_∞ observer design for a quadcopter model operating in an adaptive vertical farm," *IFAC-PapersOnLine*, vol. 56, no. 2, pp. 10837–10842, 2023, doi: 10.1016/j.ifacol.2023.10.757.

[57] F. Snobar, J. Reinhard, H. Huber, M. Hoffmann, M. Stelzig, M. Vossiek, and K. Graichen, "Fov-based model predictive object tracking for quadcopters," *IFAC-PapersOnLine*, vol. 55, no. 27, pp. 13–18, 2022, doi: 10.1016/j.ifacol.2022.10.481.

[58] H. Chen and H. Bai, "Incorporating thrust models for quadcopter wind estimation," *IFAC-PapersOnLine*, vol. 55, no. 37, pp. 19–24, 2022, doi: 10.1016/j.ifacol.2022.11.155.

[59] B. A. Iza, Q. A. Fiddina, H. N. Fadhilah, D. K. Arif, and Mardlijah, "Automatic guided vehicle (agv) tracking model estimation with ensemble kalman filter," in *AIP Conference Proceedings*, vol. 2641, no. 1, 2022, doi: 10.1063/5.0118817.

[60] R. Yadav, M. Manas, and R. K. Dubey, "Enhanced accuracy in state-of-charge estimation for lithium-ion batteries in electric vehicles using augmented adaptive extended kalman filter," *e-Prime-Advances in Electrical Engineering, Electronics and Energy*, vol. 10, 2024, doi: 10.1016/j.prime.2024.100868.

[61] L. Ma, W. Li, C.-J. Wong, J. Bao, M. Skyllas-Kazacos, B. Welch, N. Ahli, M. Faraj, and M. Mahmoud, "h_∞-extended kalman filter for the aluminium smelting process with boundness analysis of the estimation error matrix," *Control Engineering Practice*, vol. 164, 2025, doi: 10.1016/j.conengprac.2025.106500.

[62] J. Yu, A. K. J. Al-Nussairi, M. H. Chyad, N. S. S. Singh, H. Azarinfar, L. S. Munshid, Y. Liu, and W. Huang, "How can artificial networks enhance second-order hybrid extended kalman filtering for energy management?" *Energy Reports*, vol. 14, pp. 1368–1391, 2025, doi: 10.1016/j.egyr.2025.07.014.

[63] X. Lu, M. Chen, and Y. Tian, "Accurate state-of-charge estimation of lifepo4 battery: An adaptive extended kalman filter approach using particle swarm optimization," *Energy Reports*, vol. 14, pp. 1169–1178, 2025, doi: 10.1016/j.egyr.2025.07.023.

[64] L. E. di Grazia, M. Mattei, and A. Pironti, "An extended kalman filter approach for tokamak plasma equilibrium reconstruction," *Fusion Engineering and Design*, vol. 220, 2025, doi: 10.1016/j.fusengdes.2025.115363.

[65] C. O. Omeje, A. O. Salau, and C. U. Eya, "Dynamics analysis of permanent magnet synchronous motor speed control with enhanced state feedback controller using a linear quadratic regulator," *Heliyon*, vol. 10, no. 4, 2024.

[66] W. Wang, Y. Ning, Y. Zhang, P. Xu, and B. Li, "Linear active disturbance rejection control with linear quadratic regulator for stewart platform in active wave compensation system," *Applied Ocean Research*, vol. 156, 2025, doi: 10.1016/j.apor.2025.104469.

[67] Z. Su, H. Yao, J. Peng, Z. Liao, Z. Wang, H. Yu, H. Dai, and T. C. Lueth, "Lqr-based control strategy for improving human–robot companionship and natural obstacle avoidance," *Biomimetic Intelligence and Robotics*, vol. 4, no. 4, 2024, doi: 10.1016/j.birob.2024.100185.

[68] E. Çinar and T. Abut, "Fuzzy lqr-based control to ensure comfort in hvac system with two different zones," *Case Studies in Thermal Engineering*, vol. 73, 2025, doi: 10.1016/j.csite.2025.106544.

[69] J. Vasara and I. Selek, "An analysis of an lqr design for a hybrid power plant's load-sharing problem," *IFAC Journal of Systems and Control*, vol.33, 2025, doi: 10.1016/j.ifacsc.2025.100327.

[70] W. Byrski, M. Drapała, J. Byrski, M. Noack, and J. Reger, "Comparison of lqr with mpc in the adaptive stabilization of a glass conditioning process using soft-sensors for parameter identification and state observation," *Control Engineering Practice*, vol. 146, 2024, doi: 10.1016/j.conengprac.2024.105884.

[71] G. Gao, L. Xu, T. Huang, X. Zhao, and L. Huang, "Reduced-order observer-based lqr controller design for rotary inverted pendulum," *Computer Modeling in Engineering & Sciences (CMES)*, vol. 140, no. 1, 2024, doi: 10.32604/cmes.2024.047899.

[72] S. Vijayakumar and N. Sudhakar, "Design and implementation of golden eagle optimized cascaded pi and lqr controller for pfc sepic converter in ev charging," *Results in Engineering*, vol. 24, 2024, doi: 10.1016/j.rineng.2024.102942.

[73] U. Kruthika and S. Paneerselvam, "Enhanced set-point tracking in a boiler turbine system via decoupled mimo linearization and comparative lqr-based control strategy," *Results in Engineering*, vol. 25, 2025, doi: 10.1016/j.rineng.2025.103914.

[74] G. Nethaji and J. Kathirvelan, "Performance comparison between pid and fuzzy logic controllers for the hardware implementation of traditional high voltage dc-dc boost converter," *Heliyon*, vol. 10, no. 17, 2024.

[75] T. Hägglund and J. L. Guzmán, "Give us pid controllers and we can control the world," *IFAC-PapersOnLine*, vol. 58, no. 7, pp. 103–108, 2024, doi: 10.1016/j.ifacol.2024.08.018.

[76] V. R. Nippatla and S. Mandava, "Performance analysis of permanent magnet synchronous motor based on transfer function model using pid controller tuned by ziegler-nichols method," *Results in Engineering*, vol. 26, 2025, doi: 10.1016/j.rineng.2025.105460.

[77] X. Wang, "Oral english pronunciation evaluation system based on pid algorithm," *Procedia Computer Science*, vol. 261, pp. 1043–1049, 2025, doi: 10.1016/j.procs.2025.04.683.

[78] G. Si, R. Zhang, and X. Jin, "Path planning of factory handling robot integrating fuzzy logic-pid control technology," *Systems and Soft Computing*, vol. 7, 2025, doi: 10.1016/j.sasc.2025.200188.

[79] L. A. Cantera-Cantera, M. C. Maya-Rodríguez, S. I. Palomino-Resendiz, Y. Lozano-Hernández, and L. Luna, "Level and flow systems identification of an industrial processes module by lsod method for pid controllers design," *Results in Engineering*, vol. 25, 2025, doi: 10.1016/j.rineng.2025.104347.

[80] D. Zhan, A.-Q. Tian, and S.-Q. Ni, "Optimizing pid control for multi-model adaptive high-speed rail platform door systems with an improved metaheuristic approach," *International Journal of Electrical Power & Energy Systems*, vol. 169, 2025, doi: 10.1016/j.ijepes.2025.110738.